EXPERIMENTAL ANALYSIS OF SMALL MASONRY PANELS SUBJECT TO LONG DURATION BLAST LOADING

Richard A. Keys[1*], Simon K. Clubley[2]

[1*]Infrastructure Group, Faculty of Engineering and the Environment, University of Southampton, Southampton, UK, SO17 1BJ (r.keys@soton.ac.uk)
[2] Infrastructure Group, Faculty of Engineering and the Environment, University of Southampton, Southampton, UK, SO17 1BJ (s.k.clubley@soton.ac.uk)

Abstract

Much research has been conducted towards short duration blast loading and its interaction with structures. The positive phase duration, t^+, of a typical short duration high explosive blast is often below $t^+ = 100$ms. For the purposes of this research, long duration blast is considered to be an explosive event in which $t^+ > 100$ms. This type of blast load offers added complexity when dealing with its interaction with structures due to the high impulses, drag winds and associated dynamic pressures.

As part of an extended research study to develop a set of predictive algorithms, this paper investigates the breakage patterns and debris distribution of masonry panels subject to long duration blast loads. Experimental trials were conducted using the Air Blast Tunnel at MoD Shoeburyness, a specialised facility for long duration blast, in which two masonry panels were tested. The trials displayed varying degrees of breakage followed by a substantial debris distribution in both cases.

Keywords: Long duration, Blast, Masonry, Impulse, Breakage, Debris

INTRODUCTION

Long duration blast loads by nature have a large positive phase duration in which $t^+ > 100$ms. Such blast waves are produced by detonating large quantities of high explosives, such as the 1981 'Mill Race' trial reported by Reid [1] in which 544 tonnes of ANFO were detonated, or hydrocarbon vapour cloud detonation, such as the 2005 'Buncefield Disaster' reported by Burgen et al [2].

The work presented in this paper is part of an extended research project investigating the breakage and debris distribution of masonry panels subject to long duration blast loads. Using both experimental and numerical methods, the project aims to quantify the effects of the blast load, structural geometry and material properties on the breakage and debris distribution patterns. Previous research conducted by Keys & Clubley [3] investigated the comparative debris distribution of a masonry wall subject to a short duration blast load with $p_i \approx 110$kPa and $t^+ \approx 12{:}8$ms and a long duration blast wave with $p_i \approx 110$kPa and $t^+ \approx 200$ms. This paper investigates the breakage patterns and debris distribution of both mortared and unmortared masonry panels subject to long duration blast loading.

EXPERIMENTAL CONFIGURATION

Two experimental trials were conducted at the Air Blast Tunnel (ABT) displayed in Figure 1. The ABT is a shock tube designed to replicate large explosive events as discussed by Adams & Rose [4], located at MoD Shoeburyness on Foulness Island, UK.

Figure 1. The Air Blast Tunnel (ABT)

The two experiments comprised 1m × 2m masonry walls labelled ‘MW1’ and ‘MW2.’ The MW1 trial used unmortared Class B engineering bricks (210mm × 10mm × 65mm) with a compressive strength of approximately 95Nmm^2, whilst the MW2 trial was constructed from frogged, facing, London bricks (210mm × 10mm × 65mm) with a compressive strength of approximately 40-60Nmm^2, joined by a class (ii) mortar conforming to BS:5628-1:2005 [5], with a compressive strength of approximately 60-80Nmm^2 in a 10mm bedding. Each structure was painted to improve the lighting for photography and each brick was assigned a unique number to provide insight into the individual brick distributions.

Both trials were recorded using two high speed Phantom cameras operating at 5000fps; the cameras were mounted in hardened steel boxes in the upstream and side positions with the upstream camera displayed in Figure 2(a). Endveco 8510 piezoresistive pressure transducers, shown in Figure 2(b), were used to record the static overpressures and Kulite-20D pressure transducers, shown in Figure 2(c), were used to record the dynamic pressure. Both types of gauges were placed 1m upstream from the target.

(a) **(b)** **(c)**

Figure 2. Trial Instrumentation: (a) Phantom camera support & lighting, (b) Endveco 8510 pressure transducer, (c) Kulite-20D pressure transducer

RESULTS AND DISCUSSION

The pressure histories from both the MW1 and MW2 trials, displayed in Figures 3 and 4, show a very high degree of consistency between the two ABT firings in terms of both the static overpressure and dynamic pressure profiles and peak values.

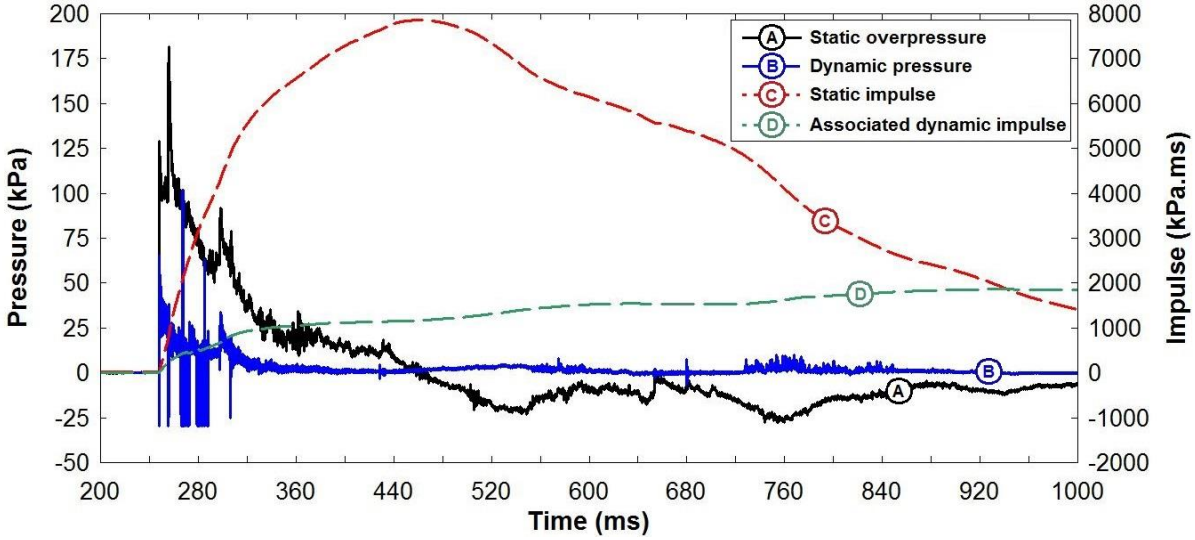

Figure 3. MW1 gauge data

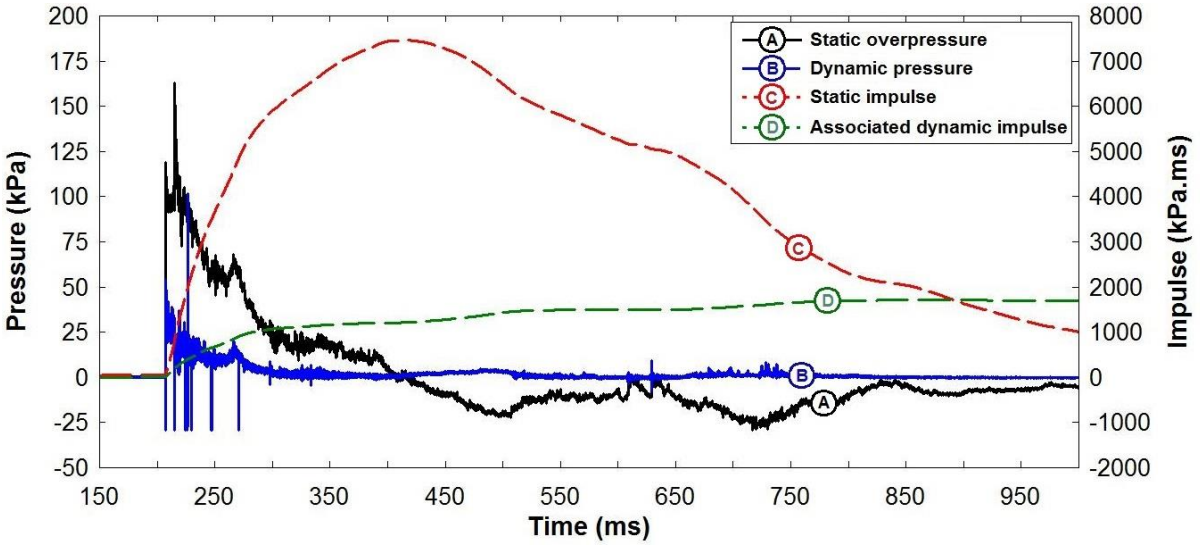

Figure 4. MW2 gauge data

The peak values recorded for the static overpressures were 181kPa for MW1 and 163kPa for MW2; a difference of 18kPa. The duration of the peak was approximately 1ms, which is negligible in terms of impulse and can potentially be due to gauge noise. The 'average peak' value for static overpressure for both trials was around 110kPa. In both cases, the positive phase duration lasted approximately 210ms, which resulted in a total transmitted impulse of 7864kPa.ms for MW1 and 7461kPa.ms for MW2. The negative phase for both trials show good consistency with a reduction in the cumulative impulse of 6437kPa.ms for MW1 and 6448kPa.ms for MW2. For both trials, the dynamic pressure readings show large fluctuations, most likely due to gauge noise. In the case of the MW1 trial, extreme fluctuations were recorded between 260ms-320ms. Notwithstanding, the total transmitted impulses due to the associated dynamic pressure from both trials offer reasonable consistency with 1886kPa.ms and 1668kPa.ms from the MW1 and MW2 trials respectively.

Both structures displayed a high level of breakage, producing extensive debris distributions. Images from the high speed photography from both MW1 and MW2 trials are shown in Figures 5 and 6 respectively.

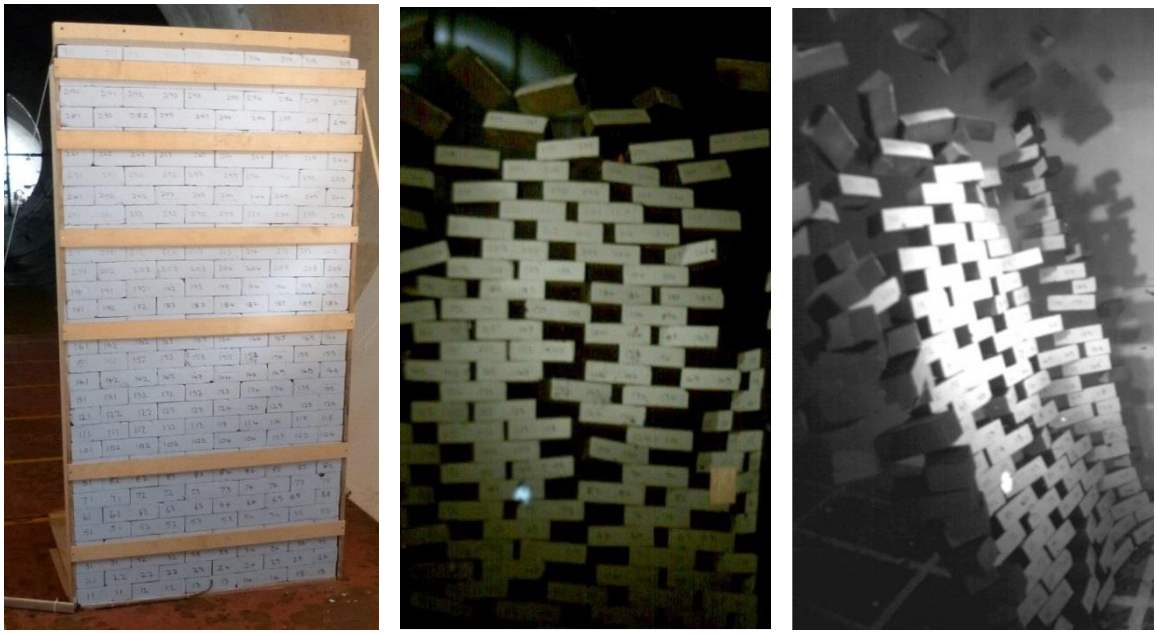

(a) **(b)** **(c)**

Figure 5. MW1 trial photography: (a) preshot - upstream perspective, (b) 100ms – upstream perspective, (c) 100ms – side perspective

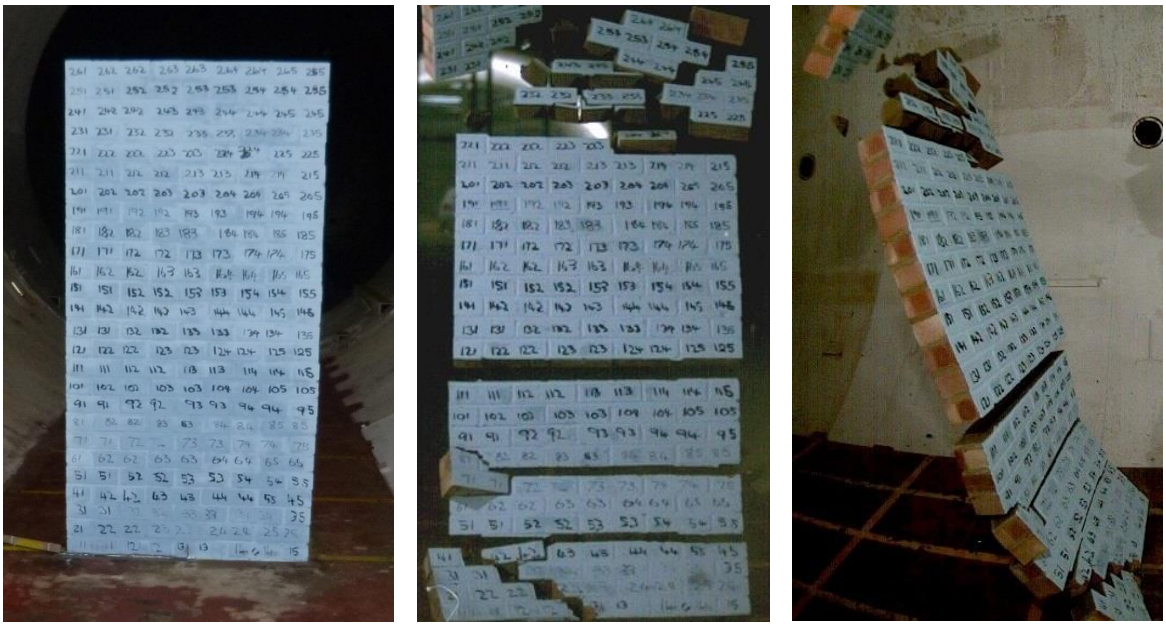

(a) **(b)** **(c)**

Figure 6. MW2 trial photography: (a) preshot - upstream perspective, (b) 100ms – upstream perspective, (c) 100ms – side perspective

Figures 5(a) and 6(a) show the MW1 and MW2 structures before firing from the upstream perspective. The wooden support framing on the MW1 structure shown in Figure 5(a) was removed before firing. The breakage pattern of the MW1 trial, displayed in Figure 5(b), shows separation of the bricks along the vertical (z) axis where the reflective pressure was highest. The reflective pressure was lowest around the edges of the structure; however, this was the weakest part of the structure, which results in increased brick separation. The breakage mechanism of the MW2 structure was simplistic by

comparison as the bedding planes of the mortar provide inherent weak points in the structure; as a result, the breakage pattern, displayed in Figure 6(b), shows four clean lines of separation along the bedding planes. Additional breakage was observed at the top of the structure where it was weakest and at the base of the structure where the reflective pressure and tilting moment were highest. Figures 5(c) and 6(c) show both structures undergo simultaneous tilting and translational movement. Analysis of the high speed photography for both trials indicate an effective velocity gradient of the initial fragments across the vertical (z) axis. Figure 7 illustrates the velocity gradients across both structures.

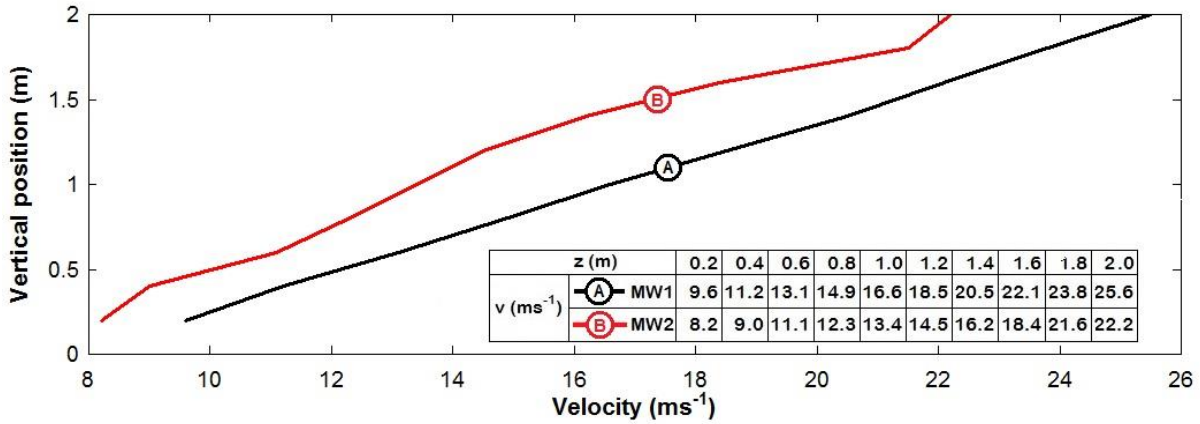

Figure 7. MW1 & MW2 initial brick velocities

The velocity gradient of MW1 was smoother than that of MW2 as the initial fragments were unrestrained, resulting in a more uniform gradient, with a total velocity range of 16ms^{-1}. The initial fragment velocities of the MW2 trial showed localised velocity gradients across the large fragments formed as a result of breakage along specific bedding planes. The range in velocities across the MW2 structure was 14ms^{-1}. The velocity gradient across the structure was a result of the increased static load from the top to the bottom of the structure, due to the increase in mass and frictional forces. The range in velocities resulted in the effective tilting of the structure which in turn dictated the point of impact with the ground and subsequent secondary breakage and debris distribution. Due to the circular cross section of the ABT, the lateral distribution of the debris was restrained for both trials; as a result, the debris data was logged in 1D longitudinal bins of length 1m along the x-axis. Figure 8 shows the longitudinal mass distribution for both MW1 and MW2. MW1 consisted of approximately 120kg of additional mass compared with MW2; for comparison between the two debris distributions, Figure 9 displays the cumulative normalised mass distribution accompanied by a summary table of the absolute cumulative distributions for both trials.

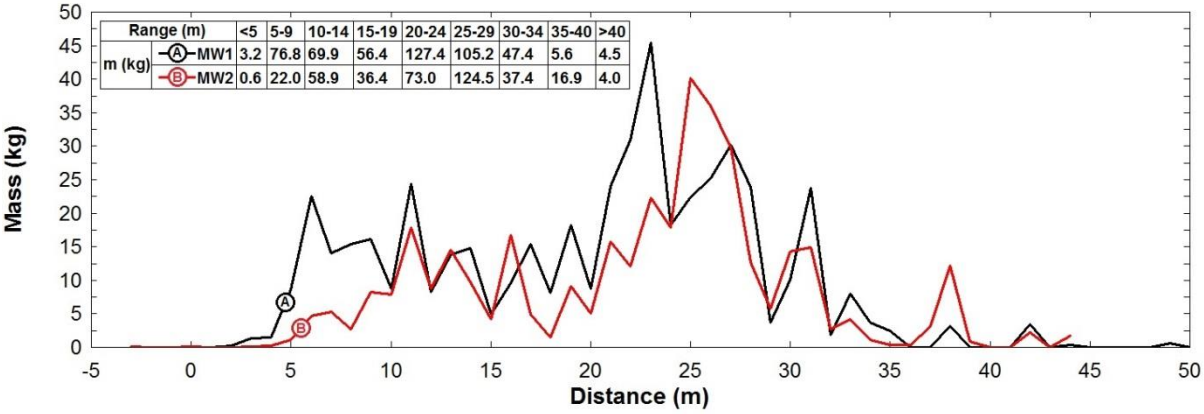

Figure 8. MW1 & MW2 longitudinal mass distribution

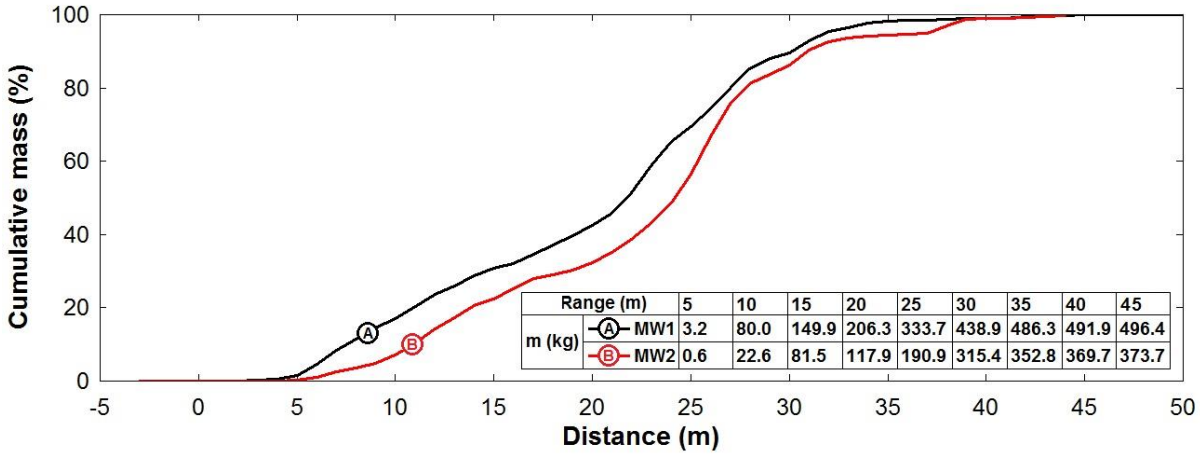

Figure 9. MW1 & MW2 longitudinal normalised cumulative mass distribution

Figure 8 shows the general shape of the debris distribution was similar in both cases, with the bulk of the mass landing within the 20m-30m range. The ABT has instrumentation columns located at approximately 31.5m from the target position; as a result of these columns, both trials showed a small peak between 30m-32m. The maximum distance was similar in both cases, with fragments located up to 44m in MW2 and up to 50m in MW1. A significantly larger portion of the mass from the MW1 trial was located between 5m-10m, which had an effect on the cumulative mass distribution, displayed in Figure 9. The shape of the cumulative distribution was similar for both trials; however, the extra mass located between 5m-10m in the case of MW1 resulted in an effective translation of the total debris distribution. Both the initial fragment velocity and the overall mass of MW1 were higher, resulting in a much higher overall momentum. This offers an explanation for the higher peak distance, but not for the reduction in the cumulative distribution. Comparison of Figures 5(b) and 6(b) show one large fragment at the base of MW2 compared to the relatively uniform breakage of MW1. The fragments from MW1 tumble and roll on impact with the ground, whereas the large fragment from MW2 slides. The launch angle from the MW2 fragment was also lower which reduces the energy dissipated to the ground and subsequent secondary fragmentation.

SUMMARY

The breakage patterns differ greatly in both trials, with MW1 showing uniform pseudo-breakage with each brick forming an individual fragment, whilst MW2 showed large initial fragments separated along bedding planes of mortar. Despite the difference in breakage patterns, initial velocities and overall mass of both structures, the debris mass distribution was similar in both cases. A detailed test specification is planned for early 2016 which will complement the MW series, specifically, the mortared MW2 trial. Utilising the same material properties of MW2, the future tests will vary the geometry and blast parameters to investigate their effects on breakage and debris distribution.

Nomenclature

Symbols		Superscripts	
I	impulse	+	positive phase
m	mass		
p	pressure		Subscripts
t	time	i	incident
v	velocity		

ACKNOWLEDGEMENTS

The authors would like to express gratitude to the UK Ministry of Defence for providing the use of testing facilities at MoD Shoeburyness. All data hereby obtained through the use of such facilities

remains the property of the UK MoD. The assistance of the Spurpark Ltd trials division is gratefully acknowledged with respect to experimental planning, instrumentation and implementation.

REFERENCES

1. Reid, G. H., "Misty castle series: Mill race event: Test execution report," Technical report, 1981, Defence Nuclear Agency.

2. B. Burgen et. al., "Buncefield explosion mechanism phase 1," Technical report, Steel Construction Institute, 2009.

3. Keys, R. A. and Clubley, S. K, *15th International Symposium on the Interaction of the Effects of Munitions with Structure*, Potsdam, Germany, October 2013.

4. Adams, L. J. and Rose, T. A., Simulating explosive events in the air blast tunnel, *22nd International Symposium on Military Aspects of Blast and Shock*, Bourges, France, November 2012.

5. British Standards Institution, BS5628-1:2005 - Code of Practice for the use of Masonry, 2005, Table 1, page 11.